JOURNAL OF VIROLOGY, Jan. 2005, p. 569–580 Vol. 79, No. 1
0022-538X/05/$08.00+0 doi:10.1128/JVI.79.1.569–580.2005

Viral Transport of DNA Damage That Mimics a Stalled Replication Fork

Jaana Jurvansuu,[1] Kenneth Raj,[1] Andrzej Stasiak,[2] and Peter Beard[1]*

Swiss Institute for Experimental Cancer Research (ISREC) and National Center of Competence in Research (NCCR) Molecular Oncology, Epalinges,[1] and Laboratory of Ultrastructural Analysis, Faculty of Biology and Medicine, University of Lausanne, Lausanne,[2] Switzerland

Received 5 June 2004/Accepted 3 August 2004

Adeno-associated virus type 2 (AAV2) infection incites cells to arrest with 4N DNA content or die if the p53 pathway is defective. This arrest depends on AAV2 DNA, which is single stranded with inverted terminal repeats that serve as primers during viral DNA replication. Here, we show that AAV2 DNA triggers damage signaling that resembles the response to an aberrant cellular DNA replication fork. UV treatment of AAV2 enhances the G_2 arrest by generating intrastrand DNA cross-links which persist in infected cells, disrupting viral DNA replication and maintaining the viral DNA in the single-stranded form. In cells, such DNA accumulates into nuclear foci with a signaling apparatus that involves DNA polymerase delta, ATR, TopBP1, RPA, and the Rad9/Rad1/Hus1 complex but not ATM or NBS1. Focus formation and damage signaling strictly depend on ATR and Chk1 functions. Activation of the Chk1 effector kinase leads to the virus-induced G_2 arrest. AAV2 provides a novel way to study the cellular response to abnormal DNA replication without damaging cellular DNA. By using the AAV2 system, we show that in human cells activation of phosphorylation of Chk1 depends on TopBP1 and that it is a prerequisite for the appearance of DNA damage foci.

The human adeno-associated virus type 2 (AAV2) can perturb cell cycle progression (51, 71) and mediate specific killing of p53-deficient cells (51). Cells with intact p53 activity were able to arrest with 4N DNA content, whereas cells without functional p53 were not able to sustain this arrest and died. This effect was shown to depend not on the viral capsid proteins or other virus-encoded proteins but on the presence of the viral DNA. The AAV2 particle contains a single-stranded DNA molecule of 4.7 kb flanked by identical inverted terminal repeats which form T-shaped hairpin structures (5). The inverted terminal repeats are thought to function as primers for viral DNA replication. The hairpin structures of AAV2 DNA together with its single strandedness were hypothesized (51) to induce DNA damage signaling after AAV2 infection. In the work presented here, we set out to test this hypothesis, to identify proteins that recognize AAV DNA, and to elucidate how these proteins then activate the pathway that leads to G_2 arrest.

An appropriate cellular response to DNA damage is crucial for maintenance of normal cell fate. Ataxia-telangiectasia-mutated (ATM) and ataxia-telangiectasia- and Rad3-related (ATR) proteins are the two major signaling kinases that respond to DNA damage in cells. The functions of these two phosphatidylinositol 3-like kinases partially overlap, but an emerging picture is that ATR is essential for cell survival due to its role in surveillance of DNA replication (8, 13, 14, 17, 19, 30, 46). In contrast, ATM is not vital to cells even though it is pivotal for normal checkpoint responses in all phases of the cell cycle (reviewed in reference 33). A major difference between these two kinases may also be the way they respond to DNA damage: ATR kinase activity has not been observed to increase with DNA damage, yet ATR seems to act specifically at sites of DNA lesions in a complex with associated proteins (66). In contrast, DNA-damaging treatments do increase ATM kinase activity, and furthermore, this has been suggested to occur even without the binding of ATM to the lesion (2, 24).

There is increasing evidence that ATR-dependent DNA damage signaling needs the functions of several other proteins in parallel to phosphorylate the main effector kinase Chk1 (15, 32, 56, 70, 81). ATR forms a complex with the ATR-interacting protein (ATRIP), which then recognizes replication protein A (RPA)-covered single-stranded DNA, thus making single-stranded DNA the primary DNA damage lesion for ATR (16, 78, 84). However, the ATR/ATRIP/RPA complex alone is not enough to activate proper downstream signaling; yet another protein complex composed of the Rad9/Rad1/Hus1 (9-1-1) proteins is needed (3, 53, 70). The 9-1-1 protein complex has a trimeric ring structure similar to that of proliferating cell nuclear antigen (10, 64, 67) and is loaded onto DNA by Rad17 complexed with replication factor C proteins (4, 27). Interestingly, ATR and Rad17 bind DNA independently, although both seem to require RPA in order to do so (34, 45, 83). The 9-1-1 complex and Rad17 have also been implicated in supervising DNA replication, and it has been suggested that Rad17 is not recruited onto chromatin specifically in response to DNA damage but is constitutively chromatin bound (50, 54).

Several proteins have been associated with the response to stalled replication forks, although their precise mode of action is somewhat obscure. Rad9 has been shown to bind topoisomerase II-binding protein 1 (TopBP1), which is similar to the yeast S-phase checkpoint protein Cut5/Rad4 (1, 39, 41, 69, 76). The Brca1 carboxyl-terminal repeat (BRCT)-containing TopBP1 is needed to establish full DNA damage-induced G_2

* Corresponding author. Mailing address: Swiss Institute for Experimental Cancer Research, Epalinges, Lausanne CH-1066, Switzerland. Phone: 41-21-692-5921. Fax: 41-21-652-6933. E-mail: Peter.Beard@isrec.ch.

arrest, and its absence, when combined with a Brca1-negative background, inhibits the G_2 arrest, suggesting that these two proteins partially compensate for each other (74, 75). BRCT domains were shown to be needed to recognize phosphopeptides (11, 40, 52, 79). Brca1 itself has been studied extensively and has been shown to be an important target of ATR and ATM kinases in activating S and G_2/M checkpoints; it is also needed for phosphorylation of several other ATM and ATR kinase targets, including Chk1 (22, 24, 66, 73). Thus, it was proposed by Foray et al. (22) that Brca1 would function as a scaffold protein to enable ATM/ATR kinases to phosphorylate proteins that are not chromatin bound, an analogous role having been described for Cut5/Rad4 in yeast and in *Xenopus* egg extracts (28, 49). However, the precise nature of the DNA structures that are recognized by sensors to activate checkpoint signaling remains unclear.

An intriguing property of DNA damage repair and signaling proteins is that they accumulate into nuclear foci after induction of DNA damage. The function of this accumulation is not clear, although it has been thought to mark the sites of DNA damage and perhaps aid the signaling and repair of DNA lesions. The formation of protein foci is a dynamic process and has been a precious tool to study the processes and proteins involved in DNA repair and signaling (20, 21, 38, 42, 43). Some of the proteins shown to accumulate onto stalled replication forks include ATR, the Mre11/NBS1/Rad50 complex, Bloom's syndrome protein (BLM), single-stranded DNA-binding proteins Rad51 and RPA, the 9-1-1 complex, Rad17, Brca1, and TopBP1 (6, 23, 26, 59, 61, 77). In yeast, it was shown by using site-specific DNA-binding proteins and unique restriction enzymes that the repair protein foci do indeed colocalize with the induced double-strand breaks and, moreover, that these foci contain more than one break (36).

The requirement for two independent protein complexes (ATR and 9-1-1) and several auxiliary proteins has been thought to be a fail-safe mechanism to prevent inappropriate activation of the DNA damage checkpoint. Here, we describe a system that tricks this fail-safe mechanism by viral transport of DNA damage. AAV2 induces cell cycle arrest in G_2. If the virus is UV treated, replication of the AAV2 DNA by polymerase delta is blocked, and this enhances the DNA damage response, manifested by Chk1 phosphorylation, and the subsequent G_2 arrest. A protein complex composed of ATR, DNA polymerase delta, TopBP1, BLM, Brca1, phosphorylated Rad17, Rad51, and RPA accumulates together with AAV2 DNA to form nuclear foci. Inhibition of DNA damage signaling through expression of kinase-dead ATR (kd-ATR) totally abolishes focus formation by the proteins and the viral DNA, Chk1 phosphorylation, and G_2 arrest. The G_2 arrest is also inhibited in cells that lack the BLM protein and in cells with reduced amounts of Rad9, TopBP1, or Chk1 protein. The results suggest that in this system, focus formation and signaling are dependent on the function of ATR and Chk1 kinases which in turn are dependent on stalled replication fork checkpoint proteins. Thus, a consequence of this study is the establishment of a well-characterized system to study damage signaling strictly dependent on ATR kinase function in mammalian cells without sacrificing cell viability.

MATERIALS AND METHODS

Cell lines. The osteosarcoma cell line U2OS was maintained in Dulbecco's modified Eagle's medium (DMEM), 5% fetal calf serum (FCS), penicillin, streptomycin, and ciprofloxacin (Ciproxin; Bayer). 293T cells were cultured in DMEM, 10% FCS, and antibiotics. The kinase-dead ATR-inducible U2OS cell line GK41 was cultured and doxycycline induced as described previously by Nghiem et al. (46); ATM-deficient (AT22IJE-T pEBS7) and ATM-complemented (AT22IJE-T pEBS7-YZ5) cell lines were described previously by Ziv et al. (82); Brca1-defective and -complemented HCC1937 cell lines were described by Scully et al. (59, 60); BLM-defective (PSNG13) and BLM-complemented (PSNF5) GM08505 cell lines were described previously by Gaymes et al. (25). NBS1-LB1 cell lines (35) were maintained in DMEM, 20% FCS plus antibiotics, and the NBS1-complemented cells with additional puromycin (10 μg/ml).

AAV2 infection, short interfering (siRNA) expression, and other cell treatments. AAV2 virus stock was a generous gift from Joan Hare (Institute of Molecular Biophysics, Tallahassee, Fla.). CsCl gradient-purified virus was dialyzed against phosphate-buffered saline (PBS) and titrated on HeLa cells by using the infectious center assay (57) but with a digoxigenin-labeled AAV2 probe (described below). UV treatment of virus was done in 50 μl of PBS in the UV Stratalinker 2400 (Stratagene) at 240 mJ/cm^2. Virus infection was performed with a small amount of plain DMEM for 4 h. The amount of virus used was dependent on the susceptibility of the particular cell line and the type of experiment and was between 500 and 50,000 particles per cell.

siRNA sequences were ordered from MGW Biotech AG and ligated into pSuper vector (9) with a puromycin selection cassette introduced to make the pSuper-Puro vector, a gift from P. Reichenbach. The sequences for siRNA were as follows: 5′-ACCCAGAAGACCTCCGAGA-3′ for UV-DDB2 and 5′-GTGG TTGTAACAGCGCATC-3′ for TopBP1. Chk1 and Rad9 siRNA target sequences were described previously (31, 55, 72). For Chk1, the two siRNA sequences were used as a mixture. 293T cells were transfected with pSuper-puro-short hairpin RNA constructs by using Lipofectamine 2000 (Life Technologies) according to the manufacturer's protocol and selected for 3 days with puromycin (3 μg/ml) before infection with AAV2 at a multiplicity of infection (MOI) of 1,000. Puromycin selection (1.5 μg/ml) was continued until cells were collected for fluorescence-activated cell sorter (FACS) analysis or Western blotting 1 day postinfection. UV treatment of cells was done with the Stratalinker, and gamma irradiation was done with an irradiator using ^{137}Cs. Fluorescence-activated cell sorting using propidium iodide was done as described previously (51).

Immunofluorescent staining of proteins and in situ hybridization. For immunofluorescence experiments, cells were plated onto coverslips a day before AAV2 infection. Two days after virus infection, cells were washed with PBS and fixed with 5% Formalin–PBS for 10 min. After fixation, cells were washed with PBS and blocked in 5% milk–1% FCS–0.1% Tween 20–PBS for 30 min. Cells were then incubated with primary antibodies in 5% milk–PBS for 30 to 60 min, after which they were washed with PBS and incubated with fluorescein-conjugated secondary antibodies in 5% milk–PBS for 30 to 60 min. Coverslips were washed with PBS containing DAPI (4′,6′,diamidino-2-phenylindole) for 1 min, washed with PBS and then water, and finally mounted onto Dabco-glycerol.

Antibodies used were anti-ATR (PC538; Oncogene Research), anti-BLM (ab476; Abcam), anti-Brca1 (sc-6954; Santa Cruz Biotechnology), anti-Flag (F3165; Sigma), anti-Rad51 (sc-8349; Santa Cruz Biotechnology), anti-phospho-Ser645-Rad17 (ab3620; Abcam), anti-RPA34 (NA18; Oncogene Research), and anti-TopPB1 (611875; BD Transduction Laboratories). Secondary fluorescent antibodies (Alexa Fluor 488 and Cy3 conjugates) used in this study were purchased from Jackson ImmunoResearch and Molecular Probes.

For colocalization of protein foci and DNA of UV-treated AAV2 (UV-AAV2 DNA), cells were plated onto gridded coverslips (CELLocate; Eppendorf). Protein immunofluorescence was done first as described above, and in situ hybridization was done immediately after the immunofluorescence results were recorded. The detailed protocol for in situ hybridization with digoxigenin-labeled probes is described in the Nonradioactive In Situ Hybridization Application Manual available at the Roche website (http://www.roche-applied-science.com/prod_inf/manuals). In short, infected cells were fixed with methanol and acetone 2 days postinfection. Cells were then treated sequentially with RNase A and pepsin and dehydrated in ethanol. The AAV2-specific probes were made by PCR using the following four AAV2-specific primer sets: 5′-AGCCTCGAACGACA ATCACT-3′ and 5′-TGCGTGACCTCTTTGACTTG-3′; 5′-AAGGGGATTAC CTCGGAGAA-3′ and 5′-GGGGATCGTACCCGTTTAGT-3′; 5′-CAAGTAC CTCGGACCCTT-3′ and 5′-CTTTTTCGCCTGGAAGACTG-3′; and 5′-CGG GGTTTTACGAGATTGTG-3′ and 5′-CACGTGCATGTGGAAGTAGC-3′ with digoxigenin-11-dUTP (Roche) in the PCR with *rTaq* DNA polymerase (Amersham Bioscience). Coverslips were hybridized at 37°C overnight with 0.3

μl of digoxigenin-labeled AAV2 PCR probe mixture in 10 μl of hybridization solution. After hybridization, the samples were washed with 2× SSC (1× SSC is 0.15 M NaCl plus 0.015 M sodium citrate) for 2 h at 56°C. Cells were blocked with 5% milk–1% NP-40–2× SSC, after which immunofluorescent staining of cells was carried out as described above by using antidigoxigenin primary antibody (clone 1.71.256; Roche). An Axioskop Coolview charge-coupled device microscope was used to detect immunofluorescent staining of proteins and DNA.

Western and Southern blots. Western blotting for phospho-serine-345-Chk1 was done exactly as described in the manufacturer's protocol (protocol number 2341; Cell signaling Technology). An ECL kit (Amersham Bioscience) was used for detection. Southern and slot blots using digoxigenin-AAV2 probes (described above) were done according to the DIG Application Manual from Roche (http://www.roche-applied-science.com/prod_inf/manuals). DNA was collected with a DNeasy tissue kit (QIAGEN). For slot blots to compare the processing of UV-AAV2 DNA in kd-ATR-inducible cells, the total amount of isolated DNA was blotted, whereas for the U2OS cell slot blot and Southern blots, 10 μg of total DNA was used. Alkaline agarose gel electrophoresis was done according the protocol described by Sambrook et al. (58).

Electron microscopy. DNA was isolated from UV-treated AAV2 with a DNeasy kit (QIAGEN) and suspended in Tris-EDTA buffer at a concentration of 100 μg/ml. Formation of RecA-single-stranded DNA complexes and the negative-staining procedure for electron microscopy are described by Sogo et al. (62). Images were recorded with a Gatan digital camera installed on a Philips CM100 electron microscope.

RT-PCR. Electronic pipettes (Biohit) were used for accuracy. Cytoplasmic mRNA was isolated by using an RNeasy mini kit (QIAGEN) and reverse transcribed with a Moloney murine leukemia virus reverse transcriptase H-point mutant (Promega) and random primers (Promega) as suggested by the manufacturer. A FastStart DNA Master SYBR Green I kit (LightCycler; Roche) was used for LightCycler PCR according to manufacturer's instructions, with 3 mM $MgCl_2$ in all the reactions. Primers for reverse transcription (RT)-PCR were 5′-GCTCTGGAATTTTGGCATCAA-3′ and 5′-TCTGAGCTGGCAAAAACTCGT-3′ for UV-DDB2 and 5′-ACGAGCTCTACCTGGAACCCT-3′ and 5′-TGCCTGGTATTGCTGGAAGAA-3′ for Rad9. Chk1 (S7) and TopBP1 primers have been described previously (29, 80). The program for all the primer pairs was the same (a denaturation step of 95°C for 10 min; an amplification step of 50 cycles of 95°C for 15 s, 66°C for 7 s, and 72°C for 10 s; and a melting step at 70 to 95°C, all with a 20°C/s slope), except that the elongation step was 18 s for TopBP1 primers.

Chromatin immunoprecipitation was done essentially as described by Abcam protocols (http://www.abcam.com/index.html?pagecontig=view_protocol&pid=171). In short, 2×10^7 U2OS cells were plated and infected with UV-AAV2 at an MOI of 5,000. Two days postinfection, cells were formalin fixed, sonicated, and precleared with protein A/G beads. Supernatants were divided into five equal fractions and incubated overnight with antibodies against RPA34 (NA18; Oncogene Research), DNA polymerase alpha (sc-5921; Santa Cruz Biotechnology), DNA polymerase epsilon (ab3163; Abcam), and DNA polymerase delta (sc-10784; Santa Cruz Biotechnology) or without antibodies. Protein-DNA complexes were collected with protein A/G beads, and samples were washed extensively, eluted, and un-cross-linked. DNA was isolated by phenol-chloroform extraction, precipitated, and slot blotted onto nylon membranes. Hybridization with AAV2-specific probes was done as described above.

RESULTS

Structure of UV-treated AAV2 DNA and its stability in cells. AAV2 has been shown to kill p53-deficient cells without the virus replicating in these cells, whereas cells with functional p53 were arrested in the G_2 phase of the cell cycle. When the virus was inactivated by treatment with UV light to ensure that it could not express any viral proteins, surprisingly, the G_2 arrest was even stronger (data not shown). These results suggested firstly that the G_2 arrest was indeed dependent solely on viral DNA and secondly that the UV treatment stabilized a structure in AAV2 DNA which was recognized by DNA damage-signaling machinery. UV-treated AAV2 was therefore analyzed further. To examine the structure of UV-AAV2 DNA, the DNA was extracted and deproteinized before complex formation with bacterial RecA protein. RecA coating of single-stranded AAV2 DNA was performed to remove potential secondary structures (63). From the electron microscopy images obtained (Fig. 1A), it was clear that UV irradiation causes the formation of intrastrand cross-links in the single-stranded AAV2 DNA. Cross-linking is probably promoted by the compact structure into which single-stranded AAV2 DNA is packed inside the viral capsid. Alkaline agarose gel electrophoresis of UV-treated AAV2 DNA and detection using Southern blotting with AAV2-specific probes showed that this

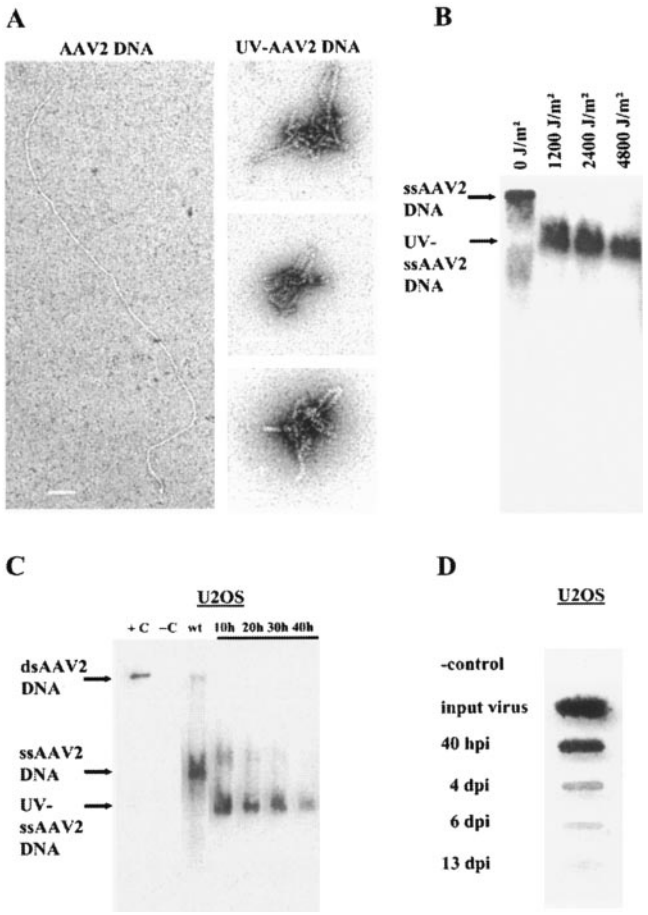

FIG. 1. UV inactivation of AAV2 causes viral DNA to form covalent intrastrand cross-links which persist in infected cells. (A) Electron microscope pictures of RecA-covered AAV2 DNA without UV treatment of virus particles (AAV2 DNA) and after UV treatment with 2,400 J/m^2 (UV-AAV2 DNA). Scale bar is 100 nm. (B) AAV2 DNAs were isolated after AAV2 virus particles were treated with the indicated amounts of UV light. Samples were Southern blotted from an alkaline agarose gel and hybridized with an AAV2-specific probe. (C) U2OS cells were infected with AAV2 or UV-AAV2 at an MOI of 5,000. Total DNA was collected 10 h postinfection for both AAV2-infected (wild type [wt]) and UV-AAV2-infected cells and was also collected for UV-AAV2-infected cells 20, 30, and 40 h postinfection. Double-stranded AAV2 DNA (+C) and total DNA from noninfected cells (−C) are controls. The replicative form of AAV2 (dsAAV2 DNA), the non-cross-linked single-stranded form (ssAAV2 DNA), and the cross-linked form (UV-ssAAV2 DNA) are indicated. (D) Total DNA was collected from UV-AAV2-infected U2OS cells at the indicated time points (days) postinfection (dpi), blotted, and probed with AAV2-specific probes. Controls include total DNA from noninfected cells (−control) and DNA isolated from virus stock (input virus).

intrastrand cross-linked DNA migrates faster than the untreated DNA, consistent with its more compact structure; it becomes more cross-linked with increasing UV doses (Fig. 1B). This experiment also revealed that the cross-linking of AAV2 DNA is alkali stable. Since the cross-links are also protease resistant, we conclude that UV treatment of AAV2 creates covalent intrastrand cross-linking in AAV2 DNA, although short peptides cannot be excluded.

When UV-AAV2 DNA was isolated from infected cells at different times, it was seen to persist as a single-stranded compact structure (Fig. 1C), showing that the virus was indeed unable to replicate. The intrastrand cross-links did not seem to be cleaved inside cells, although the UV-AAV2 DNA was slowly digested by nucleases over a period of 13 days (Fig. 1D). This processing of the DNA appears to be important for the cells to overcome the G_2 arrest (data not shown). These results suggested that the effect of UV was to stabilize AAV2 DNA in a single-stranded form unable to complete replication, although the intrastrand cross-linking did not prevent nuclease processing of the DNA.

G_2 arrest is dependent on ATR, BLM, and Rad9, but not on ATM or NBS1, proteins. To determine the proteins involved in establishment of G_2 arrest after UV-AAV2 infection, we studied cell lines deficient for different repair proteins and the corresponding lines with the deficiency complemented as well as cell lines expressing siRNA constructs. To allow a legitimate comparison of cell line pairs, they were tested to ensure equal infectibility with a recombinant AAV2-expressing luciferase protein. Human fibroblast lines defective for ATM (82), BLM (25), or NBS1; the U2OS line expressing a doxycycline-inducible kinase-dead form of ATR (13, 46, 47); and the 293T line expressing siRNA against either UV-DNA damage-binding protein 2 (UV-DDB2) or Rad9 were studied. Previous work showed that UV-treated AAV2 affects proliferation of U2OS cells infected at an MOI of 250 infectious particles per cell or more (reference 51 and data not shown). The time of G_2 arrest was proportional to the amount of virus used. The cells listed above were infected with an MOI of 500 to 5,000 infectious viral particles per cell, with the exact amount of virus used being dependent on the sensitivity of the particular cell line to the virus. Cell cycle profiles of infected and control cells were ascertained by propidium iodide FACS analysis at either 1 day postinfection for siRNA experiments or 3 days postinfection for the stable cell lines.

U2OS cells that were induced to express kd-ATR did not arrest in G_2 upon UV-AAV2 infection, while the noninduced counterpart did arrest (Fig. 2A). Moreover, the kd-ATR-expressing cells continued to cycle normally after infection, while the noninduced U2OS cells arrested with 4N DNA 12 h after infection. Cells without functional ATM reacted to UV-AAV2 infection similarly to the ATM-complemented line; that is, they arrested in G_2. In addition, there were also many dying cells (cells with less than 2N DNA content). This finding is consistent with these cells being transformed by simian virus 40 large T antigen, which disrupts p53 function. Therefore, ATR was the major DNA damage-signaling kinase responding to UV-AAV2 DNA damage, whereas ATM kinase did not seem to have any role.

To further identify the proteins needed to generate the G_2 arrest, BLM- and NBS1-deficient cell lines were studied together with 293T cells expressing siRNAs against UV-DDB2 and Rad9 proteins (Fig. 2B). Cells compromised for the Bloom's syndrome protein were unable to react to UV-AAV2 infection and continued cycling normally. The same cell line complemented with functional Bloom's syndrome protein ac-

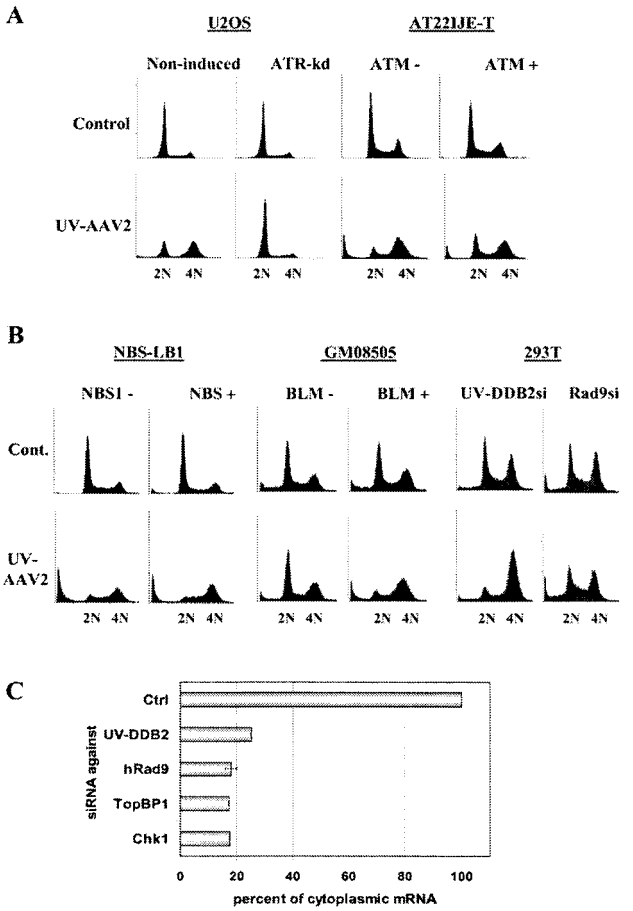

FIG. 2. UV-AAV2 infection-induced G_2 arrest is dependent on ATR, BLM, and Rad9, but not on ATM or NBS1, proteins. (A) U2OS cells not induced or doxycycline induced to express kinase-dead ATR and ATM-deficient and ATM-complemented human fibroblast cells (AT221JE-T) were infected with UV-AAV2 at an MOI of 5,000, and the cellular DNA profiles were determined by FACS analysis 3 days postinfection. For all the FACS analyses in this work, DNA profiles are shown for infected (UV-AAV2) and noninfected (Control) cells, and cellular DNA content is indicated by 2N and 4N. (B) Human transformed fibroblasts (NBS1-LB1) deficient for NBS1 protein and the complemented derivative cells were infected with UV-AAV2 at an MOI of 5,000 and collected for DNA FACS analysis 3 days after infection. The transformed human fibroblast cell line GM08505, which contains inactive BLM protein and the BLM-complemented derivative, were infected at an MOI of 50,000, and cells were collected for DNA FACS analysis 3 days postinfection. 293T cells expressing siRNAs against UV-DDB2 and Rad9 proteins were selected for 3 days, after which they were infected with UV-AAV2 at an MOI of 1,000 and collected 1 day postinfection for FACS. (C) Cells were selected for 3 days for siRNA expression, after which cytoplasmic mRNA was collected and reverse transcribed, and the produced cDNA was analyzed with real-time LightCycler PCR. Error bars are given for triplicates of one RT-PCR experiment. siRNA expression reduced the mRNA levels of UV-DDB2 by 75%, Rad9 by 82%, TopBP1 by 83%, and Chk1 by 89%. The cellular effects of siRNA expression against TopBP1 and Chk1 are shown in Fig. 5B.

cumulated with 4N DNA content and also showed higher amounts of dying cells (this line also is transformed by simian virus 40 large T antigen). siRNA directed against UV-DDB2, which is known to recognize UV lesions in DNA (65, 68), did not prevent the accumulation of G_2-arrested cells after UV-AAV2 infection, even though the siRNA reduced the amount of UV-DDB2 mRNA by 75% (Fig. 2C). In contrast, when the amount of Rad9 mRNA was reduced by 82% using siRNA, the cells' response to UV-AAV2 infection was clearly attenuated, as shown by the lack of cells accumulating in the G_2 phase. However, NBS1-defective and NBS1-complemented cell lines both responded strongly to UV-AAV2 infection, suggesting that the complex consisting of Mre11, NBS1, and Rad50 does not have a role in this G_2 arrest.

In summary, G_2 arrest is dependent on ATR kinase activity and BLM and Rad9 proteins but not on ATM, NBS1, or UV-DDB2 protein.

DNA damage-signaling proteins, DNA polymerase delta, and UV-AAV2 DNA accumulate into the same nuclear foci. After infection by UV-AAV2 (Fig. 3) or untreated AAV2 (data not shown), several DNA damage proteins accumulated into particularly distinct nuclear foci that could be seen by immunofluorescent staining of infected cells. Control immunofluorescence of noninfected cells did not show such protein focus formation. The proteins that formed nuclear foci comprised the single-stranded DNA-binding proteins Rad51 and RPA, ATR, phosphorylated Rad17, TopBP1, and Brca1. These proteins were shown to colocalize in foci, illustrated in Fig. 3 by pairwise sequential comparisons. The BLM antibody also stained specific foci that colocalized with these proteins, although this antibody also gave some prominent background staining of both uninfected and infected cells (data not shown). Figure 7 lists the proteins that colocalize into UV-AAV2-induced nuclear foci.

To test whether these proteins accumulate on UV-AAV2 DNA, we developed a sequential staining method in which immunofluorescent staining of the Rad51 protein was completed and then followed by in situ hybridization with digoxigenin-labeled AAV2-specific probes and immunofluorescence with digoxigenin-specific antibodies performed on the same cells. The patterns of Rad51 foci and the AAV2 DNA signals were very similar (for an example, see Fig. 4A), so the protein foci do colocalize with UV-AAV2 DNA. The superimposition of these two signals was not perfectly aligned because the fixation and in situ hybridization slightly altered the nuclear morphology. For in situ hybridization with AAV2 probes, samples were treated with pepsin, and both this treatment and the fixation preceding in situ hybridization were each adequate to abolish the protein foci. The secondary antibody alone did not reveal any signal after control hybridization without the digoxigenin probe (data not shown).

These results show that the protein foci, composed of ATR, TopBP1, BLM, Brca1, phospho-Rad17, RPA, and Rad51, form onto UV-AAV2 DNA, that is, onto the lesion that causes the activation of the DNA damage response. These are proteins that are implicated in cellular stalled replication fork signaling and repair. Immunofluorescent staining against the major DNA polymerases, alpha, epsilon, and delta, revealed that only polymerase delta colocalized with the nuclear protein foci formed after UV-AAV2 infection (Fig. 4B), but this was not seen with the other polymerases or in uninfected cells (data not shown). The actual binding of polymerase delta and RPA to UV-AAV2 DNA was confirmed by chromatin immunoprecipitation with detection of AAV2 DNA-specific hybridization in precipitates from cells 2 days postinfection (Fig. 4C). The results suggest that UV-induced cross-linking in AAV2 DNA stalls viral DNA replication by polymerase delta and thus leads to enhanced signaling of a defective replication fork inside infected cells.

UV-AAV2 infection induces Chk1 phosphorylation that is dependent on TopBP1. Chk1 has been shown to be the major effector kinase of the ATR kinase pathway, although ATM is also able to phosphorylate Chk1 (24). Chk1 kinase, when phosphorylated, has been shown to inhibit S and G_2/M phases of the cell cycle (37, 72). Phosphorylation of Chk1 on serine 345 was evident 1 day after UV-AAV2 infection of U2OS cells (shown in Fig. 5A). As positive controls for Chk1 phosphorylation, U2OS cells were treated with either UV irradiation (500 J/m^2), an inducer of ATR kinase activity due to blocked replication forks, or gamma rays (20 Gy). Samples treated with UV or gamma irradiation were harvested 4 h after the respective treatments. Not surprisingly, UV treatment induced heavy phosphorylation of Chk1 on serine 345 (and other sites). Twenty grays of gamma irradiation and infection with 10,000 infectious UV-AAV2 particles per cell resulted in equally intense phosphorylation of Chk1.

Brca1 protein has been shown to be needed for Chk1 phosphorylation and to establish G_2 arrest through Chk1 phosphorylation (22, 77). After UV-AAV2 infection, Brca1 was seen to colocalize with other proteins and the UV-AAV2 DNA in nuclear foci. Surprisingly, cells with nonfunctional Brca1 still appeared to react to UV-AAV2 infection (Fig. 5B), albeit less strongly than when functional Brca1 had been reintroduced into the cells. Thus, Brca1 may not be necessary for cells to react to UV-AAV2 DNA but it can sensitize the cells to it.

siRNA against another BRCT protein, TopPB1, and against the Chk1 protein independently reduced the numbers of 293T cells arrested in G_2 after UV-AAV2 infection (Fig. 5B). The expression of siRNA lowered the mRNA levels of TopBP1 and Chk1 to 17 and 11%, respectively, of controls (Fig. 2C). This result implied that these proteins are indeed needed for the establishment of DNA damage-induced G_2 arrest after UV-AAV2 infection. Interestingly, reduced amounts of either TopBP1 or Chk1 in cells resulted in a comparable slight accumulation of cells in S phase, indicating that these proteins might be in the same pathway and that the cell can still respond to some extent to UV-AAV2 DNA without these proteins. In these cells, Chk1 phosphorylation was not detectable after UV-AAV2 infection or after irradiation of cells with 20 mJ of UV irradiation/cm^2 (Fig. 5C). When siRNA against TopBP1 was expressed in Brca1-negative cells, the cells died (data not shown), an observation similar to that reported previously by Yamane et al. (74).

Chk1 phosphorylation was clearly a requirement for successful damage signaling from UV-AAV2 DNA, as its role as an effector kinase would entail. Furthermore, Chk1 is also needed for the accumulation of damage-responsive proteins into nuclear foci as shown by the lack of focus formation after UV-AAV2 infection of cells expressing siRNA against Chk1 protein (Table 1). This finding suggests that the role of Chk1 is not

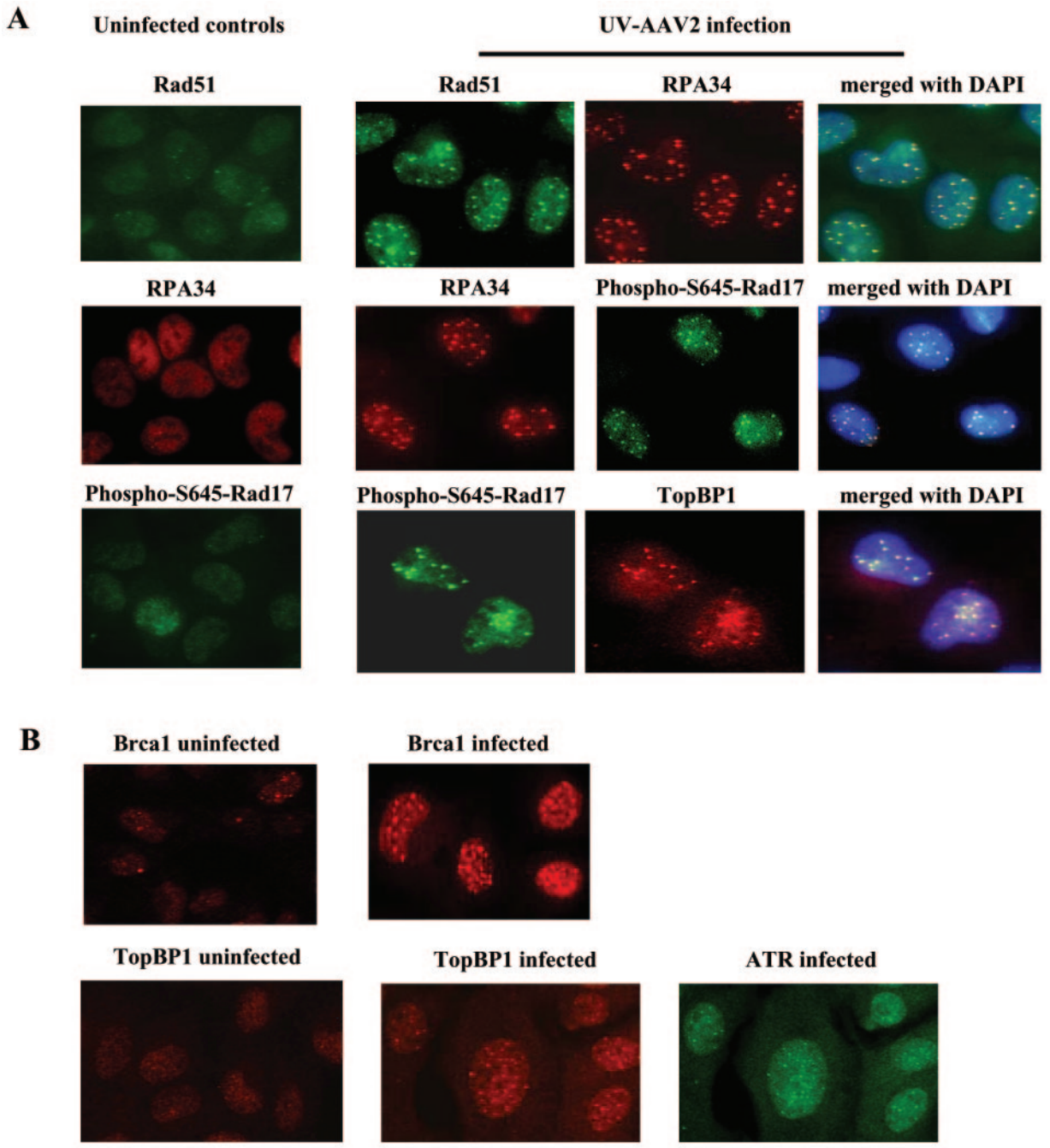

FIG. 3. DNA damage signaling and repair proteins accumulate into nuclear foci after UV-AAV2 infection. (A) Sequential pairwise colocalization of DNA damage proteins. U2OS cells were plated onto coverslips and infected with UV-AAV2 at an MOI of 10,000 (the immunofluorescence experiments needed higher input multiplicities because infections on glass coverslips seemed less efficient). Two days postinfection, cells were processed for detection of immunofluorescence with appropriate antibodies, and chromatin was stained with DAPI. UV-AAV2 infection caused Rad51, RPA34 (a subunit of RPA), serine 645-phosphorylated Rad17, and TopBP1 to colocalize in nuclear foci. Immunofluorescence of noninfected cells is shown as a control. (B) Accumulation of Brca1, TopBP1, and ATR proteins into nuclear foci.

only to signal onwards from the DNA damage but also to signal backwards to collect the DNA damage-signaling complexes into specific nuclear sites. The results demonstrate that Chk1, and its phosphorylation on serine 345, is important for protein focus formation and G_2 arrest in response to UV-AAV2 DNA damage, probably through the TopBP1 protein.

Expression of kinase-dead ATR abolishes protein-DNA foci and Chk1 phosphorylation and exposes UV-AAV2 DNA to nuclease degradation. To further study the requirement for ATR for the damage response induced by UV-AAV2 DNA, we compared the formation of protein and UV-AAV2 DNA foci, the phosphorylation of Chk1 on serine 345, and the pro-

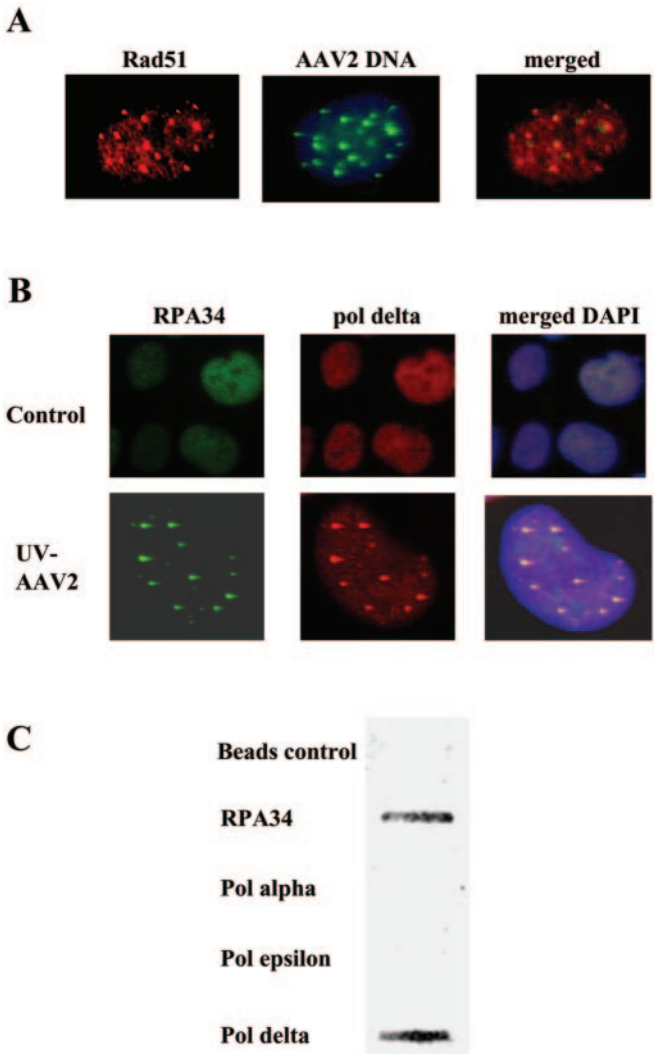

FIG. 4. UV-AAV2 DNA colocalizes with damage-responsive proteins and with DNA polymerase delta, which binds UV-AAV2 DNA directly. (A) For combined protein immunofluorescence and in situ hybridization for the viral DNA, cells were plated onto gridded coverslips and infected with UV-AAV2 as described in the legend of Fig. 3. Cells were processed 2 days postinfection as described in Materials and Methods. Rad51 protein foci, representing the proteins that form foci after UV-AAV2 infection, colocalized with UV-AAV2 DNA foci. (B) U2OS cells were plated onto coverslips and infected as described above. Two days postinfection, cells were processed for detection of immunofluorescence with antibodies against RPA and DNA polymerase (pol) delta and chromatin staining with DAPI. UV-AAV2 infection caused polymerase delta to accumulate into nuclear foci, which colocalized with RPA foci. Controls show RPA- and polymerase delta-specific staining in noninfected cells. (C) U2OS cells were infected with UV-AAV2 at an MOI of 5,000. Two days postinfection, cells were processed for chromatin immunoprecipitation as described in Materials and Methods. UV-AAV2 was immunoprecipitated without antibodies (beads control) or with antibodies against RPA (RPA34), polymerase alpha, polymerase epsilon, or polymerase delta. DNA from immunoprecipitates was slot blotted and probed with AAV2-specific probes. RPA and polymerase delta bind directly to UV-AAV2 DNA.

cessing of UV-AAV2 DNA by using U2OS cells expressing kd-ATR and the noninduced counterparts. Because expression of kd-ATR appears to render cells unable to detect the UV-AAV2 DNA, as inferred from the failure to arrest at G_2, phosphorylation of Chk1 was studied first. In kd-ATR-expressing cells, Chk1 was not phosphorylated after infection by UV-AAV2, while irradiation of these cells with UV or gamma rays did result in such phosphorylation. Thus, ATR kinase activity is strictly needed for Chk1 phosphorylation after UV-AAV2 infection, in contrast to UV and gamma irradiation, which still leads to apparent Chk1 phosphorylation in the absence of ATR activity (compare Fig. 6A with 5A).

Protein focus formation, while clear in normal U2OS cells (Fig. 3) and uninduced cells (data not shown), was abolished in U2OS cells expressing kd-ATR, which suggests that the initial ATR signaling is indispensable for the accumulation of proteins onto the area of DNA damage (Fig. 6B). Fascinatingly, UV-AAV2 DNA also failed to form foci in cells where kd-ATR expression was induced (Fig. 6C). By infection with luciferase-expressing recombinant AAV2, the cells either expressing or not expressing kd-ATR were shown to be equally well transduced; therefore, AAV2 DNA is taken up by the kd-ATR-expressing cells. Also, by slot blotting, UV-AAV2 DNA was seen to persist in kd-ATR-induced cells as described below, although it was not detectable by in situ hybridization. This finding suggested that the DNA foci seen to colocalize with the protein foci were actually composed of several UV-AAV2 DNA molecules; that is, the resolution of the in situ hybridization procedure was not sensitive enough to detect dispersed UV-AAV2 DNA molecules in infected cells.

Nuclease processing of UV-AAV2 DNA was also seen to be different if the UV-AAV2 DNA was in foci in G_2-arrested cells or present as scattered molecules in dividing cells. Total DNA was collected from all the cells on a plate and slot blotted at several time points after UV-AAV2 infection. AAV2-specific probing of the blots showed that UV-AAV2 DNA disappeared faster in cells expressing kd-ATR (Fig. 6D). Thus, protein foci, or G_2 arrest, seemed to protect the UV-AAV2 DNA inside the cells.

In summary, inhibition of ATR kinase activity in cells results in a failure to assemble proteins and DNA into nuclear foci, to activate Chk1 kinase, and to arrest in G_2 after UV-AAV2 infection.

DISCUSSION

AAV2 DNA as DNA damage substrate. This work has shown that infection by AAV2 or UV-inactivated AAV2 provokes a cellular damage response characteristic of an aberrant replication fork and that this leads to cell cycle arrest. UV treatment of AAV2 cross-links the viral single-stranded DNA to form covalent intrastrand connections which persist in infected cells. UV-treated AAV2 DNA is thus stabilized in a single-stranded form inside cells, incapable of completing replication. This enables analyses, including direct visualization of the damaged DNA by in situ hybridization and chromatin immunoprecipitation, that cannot be accomplished with other damage-signaling inducers in mammalian cells. The results show that the viral DNA provokes an ATR-mediated damage response that involves proteins characteristic of replication block signaling, including BLM, RPA, Brca1, TopBP1, and Rad9/Rad1/Hus1 but not ATM or NBS1. Using *Xenopus* egg extracts, it was shown that ATR and Hus1 bind single-stranded DNA in an RPA-dependent manner (17, 34, 78). This result is consistent

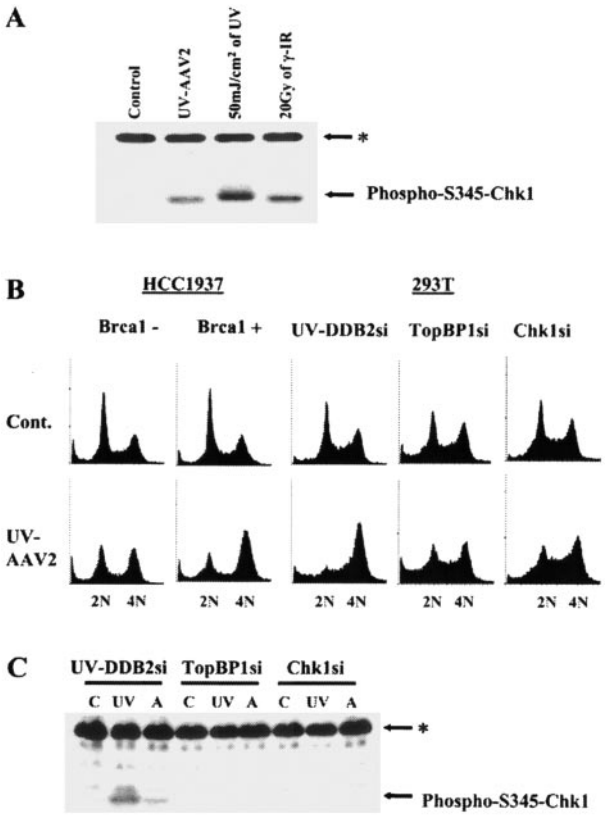

FIG. 5. Phosphorylation of Chk1 protein is needed for proper establishment of G_2 arrest after UV-AAV2 infection. (A) U2OS cells were infected with UV-AAV2 as described in the legend of Fig. 3, and proteins were collected for phospho-S345-Chk1 Western blot 1 day postinfection (UV-AAV2). For controls, proteins were collected from nontreated U2OS cells (Control) and cells treated with 50 mJ of UV irradiation/cm^2 and 20 Gy of gamma irradiation (γ-IR) 4 h after respective treatments. * denotes an unspecific band. (B) The breast carcinoma cell line HCC1937 expressing truncated Brca1 and the functional Brca1-complemented cell line were infected with UV-AAV2 at an MOI of 5,000 and collected for FACS analysis 3 days postinfection. 293T cells expressing siRNAs against UV-DDB2, TopBP1, and Chk1 proteins were selected for 3 days, after which they were infected with UV-AAV2 at an MOI of 1,000 and collected 1 day postinfection for FACS analysis. Cont., control. (C) Cells expressing siRNAs against UV-DDB2, TopBP1, and Chkl were either untreated (C), UV irradiated with 20 mJ/cm^2 (UV), or infected with 1,000 MOI of UV-AAV2 (A), and proteins were collected for Western blot and probed with phospho-S345-Chk1 antibody. * denotes an unspecific band.

with the function of ATR and the 9-1-1 complex at stalled replication forks where both single-stranded DNA and RPA are found. Therefore, UV-AAV2 DNA would be an ideal stable substrate for these proteins.

Consistent with the results of Winocour et al. (71), who also noted that both AAV and UV-inactivated AAV inhibit cell cycle progression, we found that non-UV-treated AAV2 is also able to induce formation of nuclear foci and arrest cells in G_2, although to a lesser extent than the treated virus. This damage response again likely reflects the cell's reaction to the presence of abnormal replication forks, and AAV may be able to take advantage of it. The association of AAV DNA with single-stranded DNA-binding proteins such as RPA and with Rad17, which with the PCNA-like 9-1-1 complex has been suggested to oversee DNA replication (50, 54), could stabilize replicative structures and promote synthesis of the viral DNA strands.

It has been previously reported that retroviral integration leads to an ATR-dependent DNA damage response (18). Integration of retrovirus was enhanced by ATR activity. In cells expressing kinase-dead ATR, retroviral infection led to apoptosis, possibly due to accumulation of integration intermediates. In this case, however, the consequence of inactivating ATR is quite the opposite; that is, the kinase-dead ATR-expressing cells continued to divide as if they could not detect the virus at all. This finding strongly suggests that UV-AAV2 DNA does not cause damage but is the DNA damage itself.

The actual UV lesions in UV-AAV2 DNA did not seem to play any part in this DNA damage response through being recognized directly. First, since non-UV-treated AAV2 also induces damage signaling, UV lesion-recognizing proteins cannot be solely responsible for the response seen. Secondly, the UV-DNA damage binding protein 2 was not involved in establishing G_2 arrest as assessed by siRNA-mediated knockdown of the protein, excluding a response through recognition of cyclobutane pyrimidine dimers or 6-4 photoproducts, although we cannot rule out recognition of the intrastrand crosslinks by other proteins.

Transfected single-stranded DNA oligonucleotides of various lengths have been shown to induce DNA damage and apoptotic signals in an ATM- and p53-dependent manner (48), which is different from the response that we observed with AAV2. Injection of an oligonucleotide corresponding to the AAV2 hairpin with a single-stranded tail killed p53-deficient cells, whereas simple hairpin-shaped oligonucleotides did not (51; our unpublished data). Together with the results reported here, this suggests that single-stranded or hairpin DNA structure alone is not sufficient to elicit the response we see but that this response depends on additional components of the replication fork complex.

Recognition complex model. These results provide a novel means to study ATR-dependent signaling and the function of damage foci in mammalian cells. UV-AAV2 infection induces G_2 arrest that is dependent on ATR activity and the presence of BLM, Rad9, TopBP1, and Chk1 proteins. Protein that accumulated onto the AAV2 DNA foci were ATR, DNA polymerase delta, TopBP1, BLM, Brca1, phosphorylated Rad17, Rad51, and RPA34. Moreover, RPA and polymerase delta were shown to bind directly to UV-AAV2 DNA. RPA and Rad51 proteins are known single-stranded DNA-binding proteins. The RPA protein is required for binding of both ATR/ATRIP and 9-1-1 protein complexes to single-stranded DNA (34, 83). ATR is able to phosphorylate Rad17 on serines 635 and 645 in a 9-1-1 complex-dependent manner (3, 84). Thus, ATR and the 9-1-1 protein complexes are recruited indepen-

TABLE 1. siRNAs against TopBP1 or Chk1 inhibit nuclear RPA focus formation after UV-AAV2 infection[a]

siRNA against	% of cells with >3 foci	*n*
DDB2	81.7	453
TopBP1	20.5	425
Chk1	26.7	648

[a] Cells were processed for immunofluorescence 1 day postinfection.

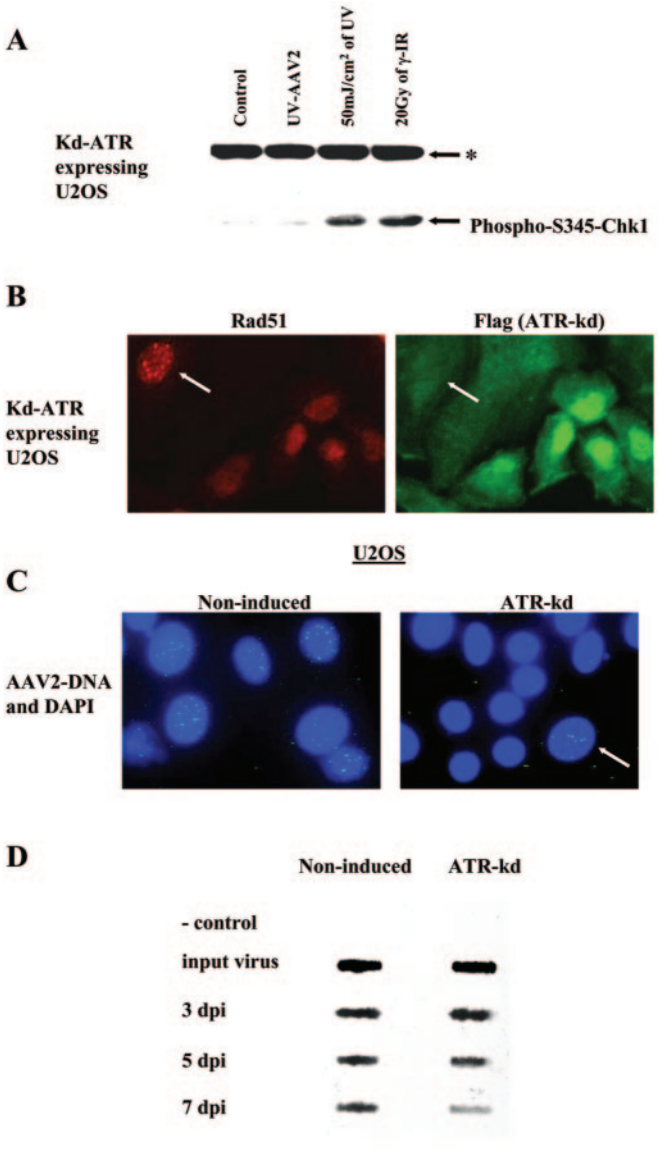

FIG. 6. Expression of kinase-dead ATR abolishes Chk1 phosphorylation, prevents the formation of protein and UV-AAV2 DNA nuclear foci, and exposes UV-AAV2 DNA to nucleases. (A) U2OS cells inducible for kd-ATR were doxycycline induced 1 day before infection with UV-AAV at an MOI of 10,000, and proteins were collected 1 day postinfection (UV-AAV2). Controls include noninfected cells (Control) and cells treated with 50 mJ of UV irradiation/cm^2 and 20 Gy of gamma irradiation (γ-IR). * denotes an unspecific band. (B) kd-ATR-expressing cells were infected with UV-AAV2 as described above and stained for immunofluorescence against Rad51 and Flag. The kd-ATR protein has a Flag tag which enables cells which were successfully induced for kd-ATR expression to be distinguished. The white arrows point out a cell that does not express Flag-tagged kd-ATR and where Rad51 still does form nuclear foci. (C) For in situ hybridization against UV-AAV2 DNA, cells were infected with UV-AAV2 and processed as described in Materials and Methods 2 days postinfection. UV-AAV2 DNA forms nuclear foci in U2OS cells but not in cells induced to express kd-ATR. The white arrow indicates an internal control cell which probably failed to express kd-ATR as judged by its cell cycle-arrested appearance (enlarged nucleus). (D) U2OS noninduced cells and cells induced to express kd-ATR were infected with UV-AAV2 at an MOI of 5,000 and were collected 3, 5, and 7 days postinfection (dpi). DNA was isolated from all the cells on a plate, and the whole yield of DNA was slot blotted and hybridized with an AAV2-specific probe. For controls, DNA was collected from noninfected cells (−control) and from an equivalent of 5,000 MOI of virus particles (input virus).

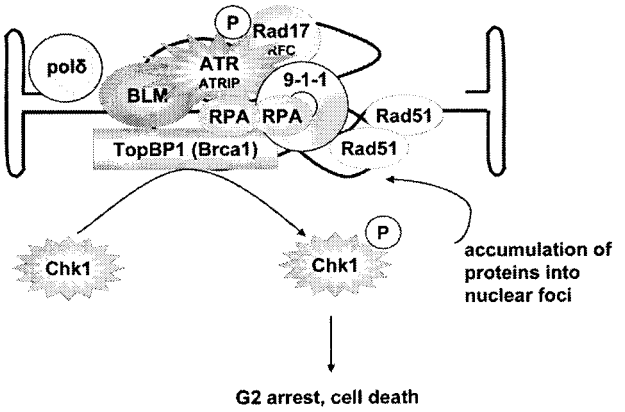

FIG. 7. Hypothetical model of UV-AAV2 DNA-recognizing proteins and signaling through Chk1. The proteins that colocalized into UV-AAV2-induced nuclear foci are ATR, BLM, Brca1, DNA polymerase delta (polδ), TopBP1, phospho-Rad17, Rad51, and RPA. See the text for details.

dently but move into close proximity to each other. The ATR and 9-1-1 complexes are hypothesized to work together on stalled replication forks enabling further recruitment of other proteins, subsequently leading to phosphorylation of Chk1 (12, 44). Our results strongly suggest that both ATR and the 9-1-1 complex are also needed to create a proper ATR kinase response after UV-AAV2 infection.

Therefore, on the basis of our own work and previously published work, we propose that the AAV2 DNA is first recognized by DNA polymerase delta and by single-stranded DNA-binding proteins RPA and Rad51. If polymerase delta is not able to finish replication of the viral DNA, RPA recruits the ATR and 9-1-1 complexes. BLM protein may be recruited by RPA or single-stranded DNA, as it has also been shown to bind and colocalize on single-stranded DNA at stalled replication forks in an ATR-dependent manner (6, 7, 23). Together, these proteins promote the ATR kinase activity and attract the adaptor proteins TopBP1 and Brca1, which facilitate the ATR-dependent phosphorylation of Chk1, leading to G_2 arrest.

The physical requirement for DNA polymerase delta in the establishment of the stalled replication fork signaling complex and the precise origin of the signal are still open questions. It is possible that the single-stranded DNA introduced by AAV is the primary signal for the virus-induced damage response. In this case, the UV-treated DNA would persist stably in the single-stranded form and induce a stronger response because replication cannot be completed. Alternatively, blocked replication could be the primary signal. If true, this would imply there are blocks, at least transiently, to replication of untreated AAV DNA. Finally a combination of a stalled fork and single-stranded DNA may give the maximal response. The presence of polymerase delta suggests that DNA synthesis has occurred, but the mere binding of the polymerase to UV-AAV2 DNA

may suffice. It is difficult to directly test the requirement for replication because DNA synthesis inhibitors themselves also induce DNA damage signaling. The UV-AAV2 DNA recognition and signaling model is depicted in Fig. 7.

Function of nuclear foci. Accumulation of proteins into nuclear foci, apparently to the sites of DNA lesions, is speculated to be necessary for the downstream signaling and for the enhanced repair of damage by concentrating repair and signaling proteins and their substrates to certain areas of the nucleus. However, these ideas have been difficult to prove or disprove. It has been shown frequently that accumulation of certain DNA damage-responsive proteins into foci depends on other proteins or the major signaling kinases. In the work reported here, we show that the proteins accumulating in the foci are indeed indispensable for signaling of DNA damage. Moreover, not only is focus formation dependent on ATR and its accessory proteins, but in addition, proper activation of the effector kinase Chk1 is a prerequisite for accumulation of protein complexes into visible foci (Table 1). The results also show that multiple copies of UV-AAV2 DNA are collected into a limited number of foci and that the repair proteins accumulate at these same foci. Thus, although nuclear foci do indicate sites of damaged DNA, they do not specify the number of lesions. This result is compatible with those from a yeast experiment in which it was shown that a protein focus colocalizes with more than one double-strand break (36). We also observed that UV-AAV2 DNA was digested faster in cells where the viral DNA did not accumulate with proteins into nuclear foci. It would make sense that DNA damage-induced protein foci are able to protect DNA inside them from nucleases in order to further ensure accurate repair.

Our work has shown that it is possible to use a virus to import strictly ATR activity-specific DNA damage into cells. The results support the model of synergistic activity of the ATR and 9-1-1 protein complexes at stalled replication forks in human cells in vivo yet outside the context of chromatin. Additionally, we were able to shed light on functions of auxiliary proteins, particularly Chk1, that assist in ATR-mediated signaling. These findings should facilitate the study of ATR-specific DNA damage-signaling processes. In summary, in this article, we have described a means to trick cells with nonmutagenic extrachromosomal DNA to initiate DNA damage signaling, which can direct checkpoint-deficient cells towards death.

ACKNOWLEDGMENTS

We are very grateful for the help of Joan Hare, Paul Nghiem, Stuart Schreiber, Manuel Stucki, Ralph Scully, Yosef Shiloh, Lovorka Stojic, Joseph Jiricny, Margaret Zdzienicka, Alicja Stasiak, Angelos Constantinou, Bernhard Hirt, Patrick Reichenbach, Nicole Paduwat, and Carin Ingemarsdotter.

This work was supported by the National Center of Competence in Research (NCCR) Molecular Oncology, a research instrument of the Swiss National Science Foundation, and Cancer Research Switzerland. A.S. acknowledges SNF grant no. 3100–058841.

REFERENCES

1. **Araki, H., S.-H. Leem, A. Phongdara, and A. Sugino.** 1995. Dpb11, which interacts with DNA polymerase II(ϵ) in *Saccharomyces cerevisiae*, has a dual role in S-phase progression and at a cell cycle checkpoint. Proc. Natl. Acad. Sci. USA **92:**11791–11795.
2. **Bakkenist, C. J., and M. B. Kastan.** 2003. DNA damage activates ATM through intermolecular autophosphorylation and dimer dissociation. Nature **421:**499–506.
3. **Bao, S., R. S. Tibbetts, K. M. Brumbaugh, Y. Fang, D. A. Richardson, A. Ali, S. M. Chen, R. T. Abraham, and X. F. Wang.** 2001. ATR/ATM-mediated phosphorylation of human Rad17 is required for genotoxic stress responses. Nature **411:**969–974.
4. **Bermudez, V. P., L. A. Lindsey-Boltz, A. J. Cesare, Y. Maniwa, J. D. Griffith, J. Hurwitz, and A. Sancar.** 2003. Loading of the human 9-1-1 checkpoint complex onto DNA by the checkpoint clamp loader hRad17-replication factor C complex in vitro. Proc. Natl. Acad. Sci. USA **100:**1633–1638.
5. **Berns, K. I., and R. M. Linden.** 1995. The cryptic life style of adeno-associated virus. Bioessays **17:**237–245.
6. **Bischof, O., S. H. Kim, J. Irving, S. Beresten, N. A. Ellis, and J. Campisi.** 2001. Regulation and localization of the Bloom syndrome protein in response to DNA damage. J. Cell Biol. **153:**367–380.
7. **Brosh, R. M., Jr., J. L. Li, M. K. Kenny, J. K. Karow, M. P. Cooper, R. P. Kureekattil, I. D. Hickson, and V. A. Bohr.** 2000. Replication protein A physically interacts with the Bloom's syndrome protein and stimulates its helicase activity. J. Biol. Chem. **275:**23500–23508.
8. **Brown, E. J., and D. Baltimore.** 2003. Essential and dispensable roles of ATR in cell cycle arrest and genome maintenance. Genes Dev. **17:**615–628.
9. **Brummelkamp, T. R., R. Bernards, and R. Agami.** 2002. A system for stable expression of short interfering RNAs in mammalian cells. Science **296:**550–553.
10. **Burtelow, M. A., P. M. Roos-Mattjus, M. Rauen, J. R. Babendure, and L. M. Karnitz.** 2001. Reconstitution and molecular analysis of the hRad9-hHus1-hRad1 (9-1-1) DNA damage responsive checkpoint complex. J. Biol. Chem. **276:**25903–25909.
11. **Caldecott, K. W.** 2003. Cell signaling. The BRCT domain: signaling with friends? Science **302:**579–580.
12. **Caspari, T., and A. M. Carr.** 2002. Checkpoints: how to flag up double-strand breaks. Curr. Biol. **12:**R105–R107.
13. **Casper, A. M., P. Nghiem, M. F. Arlt, and T. W. Glover.** 2002. ATR regulates fragile site stability. Cell **111:**779–789.
14. **Cha, R. S., and N. Kleckner.** 2002. ATR homolog Mec1 promotes fork progression, thus averting breaks in replication slow zones. Science **297:**602–606.
15. **Chini, C. C., and J. Chen.** 2003. Human claspin is required for replication checkpoint control. J. Biol. Chem. **278:**30057–30062.
16. **Cortez, D., S. Guntuku, J. Qin, and S. J. Elledge.** 2001. ATR and ATRIP: partners in checkpoint signaling. Science **294:**1713–1716.
17. **Costanzo, V., D. Shechter, P. J. Lupardus, K. A. Cimprich, M. Gottesman, and J. Gautier.** 2003. An ATR- and Cdc7-dependent DNA damage checkpoint that inhibits initiation of DNA replication. Mol. Cell **11:**203–213.
18. **Daniel, R., G. Kao, K. Taganov, J. G. Greger, O. Favorova, G. Merkel, T. J. Yen, R. A. Katz, and A. M. Skalka.** 2003. Evidence that the retroviral DNA integration process triggers an ATR-dependent DNA damage response. Proc. Natl. Acad. Sci. USA **100:**4778–4783.
19. **de Klein, A., M. Muijtjens, R. van Os, Y. Verhoeven, B. Smit, A. M. Carr, A. R. Lehmann, and J. H. Hoeijmakers.** 2000. Targeted disruption of the cell-cycle checkpoint gene ATR leads to early embryonic lethality in mice. Curr. Biol. **10:**479–482.
20. **Du, L. L., T. M. Nakamura, B. A. Moser, and P. Russell.** 2003. Retention but not recruitment of Crb2 at double-strand breaks requires Rad1 and Rad3 complexes. Mol. Cell. Biol. **23:**6150–6158.
21. **Essers, J., A. B. Houtsmuller, L. van Veelen, C. Paulusma, A. L. Nigg, A. Pastink, W. Vermeulen, J. H. Hoeijmakers, and R. Kanaar.** 2002. Nuclear dynamics of RAD52 group homologous recombination proteins in response to DNA damage. EMBO J. **21:**2030–2037.
22. **Foray, N., D. Marot, A. Gabriel, V. Randrianarison, A. M. Carr, M. Perricaudet, A. Ashworth, and P. Jeggo.** 2003. A subset of ATM- and ATR-dependent phosphorylation events requires the BRCA1 protein. EMBO J. **22:**2860–2871.
23. **Franchitto, A., and P. Pichierri.** 2002. Bloom's syndrome protein is required for correct relocalization of RAD50/MRE11/NBS1 complex after replication fork arrest. J. Cell Biol. **157:**19–30.
24. **Gatei, M., B. B. Zhou, K. Hobson, S. Scott, D. Young, and K. K. Khanna.** 2001. Ataxia telangiectasia mutated (ATM) kinase and ATM and Rad3 related kinase mediate phosphorylation of Brca1 at distinct and overlapping sites. In vivo assessment using phospho-specific antibodies. J. Biol. Chem. **276:**17276–17280.
25. **Gaymes, T. J., P. S. North, N. Brady, I. D. Hickson, G. J. Mufti, and F. V. Rassool.** 2002. Increased error-prone non homologous DNA end-joining—a proposed mechanism of chromosomal instability in Bloom's syndrome. Oncogene **21:**2525–2533.
26. **Greer, D. A., B. D. Besley, K. B. Kennedy, and S. Davey.** 2003. hRad9 rapidly binds DNA containing double-strand breaks and is required for damage-dependent topoisomerase II beta binding protein 1 focus formation. Cancer Res. **63:**4829–4835.
27. **Griffith, J. D., L. A. Lindsey-Boltz, and A. Sancar.** 2002. Structures of the human Rad17-replication factor C and checkpoint Rad 9-1-1 complexes

visualized by glycerol spray/low voltage microscopy. J. Biol. Chem. **277:** 15233–15236.
28. **Harris, S., C. Kemplen, T. Caspari, C. Chan, H. D. Lindsay, M. Poitelea, A. M. Carr, and C. Price.** 2003. Delineating the position of *rad4*$^{+}$/*cut5*$^{+}$ within the DNA-structure checkpoint pathways in *Schizosaccharomyces pombe*. J. Cell Sci. **116:**3519–3529.
29. **Haruki, N., H. Saito, Y. Tatematsu, H. Konishi, T. Harano, A. Masuda, H. Osada, Y. Fujii, and T. Takahashi.** 2000. Histological type-selective, tumor-predominant expression of a novel CHK1 isoform and infrequent in vivo somatic CHK2 mutation in small cell lung cancer. Cancer Res. **60:**4689–4692.
30. **Heffernan, T. P., D. A. Simpson, A. R. Frank, A. N. Heinloth, R. S. Paules, M. Cordeiro-Stone, and W. K. Kaufmann.** 2002. An ATR- and Chk1-dependent S checkpoint inhibits replicon initiation following UVC-induced DNA damage. Mol. Cell. Biol. **22:**8552–8561.
31. **Hirai, I., and H. G. Wang.** 2002. A role of the C-terminal region of human Rad9 (hRad9) in nuclear transport of the hRad9 checkpoint complex. J. Biol. Chem. **277:**25722–25777.
32. **Jiang, K., E. Pereira, M. Maxfield, B. Russell, D. M. Goudelock, and Y. Sanchez.** 2003. Regulation of Chk1 includes chromatin association and 14-3-3 binding following phosphorylation on Ser-345. J. Biol. Chem. **278:**25207–25217.
33. **Kastan, M. B., and D. S. Lim.** 2000. The many substrates and functions of ATM. Nat. Rev. Mol. Cell Biol. **1:**179–186.
34. **Lee, J., A. Kumagai, and W. G. Dunphy.** 2003. Claspin, a Chk1-regulatory protein, monitors DNA replication on chromatin independently of RPA, ATR, and Rad17. Mol. Cell **11:**329–340.
35. **Lee, J. H., B. Xu, C. H. Lee, J. Y. Ahn, M. S. Song, H. Lee, C. E. Canman, J. S. Lee, M. B. Kastan, and D. S. Lim.** 2003. Distinct functions of Nijmegen breakage syndrome in ataxia telangiectasia mutated-dependent responses to DNA damage. Mol. Cancer Res. **1:**674–681.
36. **Lisby, M., U. H. Mortensen, and R. Rothstein.** 2003. Colocalization of multiple DNA double-strand breaks at a single Rad52 repair centre. Nat. Cell Biol. **5:**572–577.
37. **Liu, Q., S. Guntuku, X.-S. Cui, S. Matsuoka, D. Cortez, K. Tamai, G. Luo, S. Carattini-Rivera, F. DeMayo, A. Bradley, L. A. Donehower, and S. J. Elledge.** 2000. Chk1 is an essential kinase that is regulated by Atr and required for the G_2/M DNA damage checkpoint. Genes Dev. **14:**1448–1459.
38. **Lukas, C., J. Falck, J. Bartkova, J. Bartek, and J. Lukas.** 2003. Distinct spatiotemporal dynamics of mammalian checkpoint regulators induced by DNA damage. Nat. Cell Biol. **5:**255–260.
39. **Makiniemi, M., T. Hillukkala, J. Tuusa, K. Reini, M. Vaara, D. Huang, H. Pospiech, I. Majuri, T. Westerling, T. P. Makela, and J. E. Syvaoja.** 2001. BRCT domain-containing protein TopBP1 functions in DNA replication and damage response. J. Biol. Chem. **276:**30399–30406.
40. **Manke, I. A., D. M. Lowery, A. Nguyen, and M. B. Yaffe.** 2003. BRCT repeats as phosphopeptide-binding modules involved in protein targeting. Science **302:**636–639.
41. **Marchetti, M. A., S. Kumar, E. Hartsuiker, M. Maftahi, A. M. Carr, G. A. Freyer, W. C. Burhans, and J. A. Huberman.** 2002. A single unbranched S-phase DNA damage and replication fork blockage checkpoint pathway. Proc. Natl. Acad. Sci. USA **99:**7472–7477.
42. **Maser, R. S., K. J. Monsen, B. E. Nelms, and J. H. Petrini.** 1997. hMre11 and hRad50 nuclear foci are induced during the normal cellular response to DNA double-strand breaks. Mol. Cell. Biol. **17:**6087–6096.
43. **Meister, P., M. Poidevin, S. Francesconi, I. Tratner, P. Zarzov, and G. Baldacci.** 2003. Nuclear factories for signalling and repairing DNA double strand breaks in living fission yeast. Nucleic Acids Res. **31:**5064–5073.
44. **Melo, J., and D. Toczyski.** 2002. A unified view of the DNA-damage checkpoint. Curr. Opin. Cell Biol. **14:**237–245.
45. **Melo, J. A., J. Cohen, and D. P. Toczyski.** 2001. Two checkpoint complexes are independently recruited to sites of DNA damage in vivo. Genes Dev. **15:**2809–2821.
46. **Nghiem, P., P. K. Park, Y. Kim, C. Vaziri, and S. L. Schreiber.** 2001. ATR inhibition selectively sensitizes G_1 checkpoint-deficient cells to lethal premature chromatin condensation. Proc. Natl. Acad. Sci. USA **98:**9092–9097.
47. **Nghiem, P., P. K. Park, Y.-S. Kim, B. N. Desai, and S. L. Schreiber.** 2002. ATR is not required for p53 activation but synergizes with p53 in the replication checkpoint. J. Biol. Chem. **277:**4428–4434.
48. **Nur, E. K. A., T. K. Li, A. Zhang, H. Qi, E. S. Hars, and L. F. Liu.** 2003. Single-stranded DNA induces ataxia telangiectasia mutant (ATM)/p53-dependent DNA damage and apoptotic signals. J. Biol. Chem. **278:**12475–12481.
49. **Parrilla-Castellar, E. R., and L. M. Karnitz.** 2003. Cut5 is required for the binding of Atr and DNA polymerase alpha to genotoxin-damaged chromatin. J. Biol. Chem. **278:**45507–45511.
50. **Post, S. M., A. E. Tomkinson, and E. Y. Lee.** 2003. The human checkpoint Rad protein Rad17 is chromatin-associated throughout the cell cycle, localizes to DNA replication sites, and interacts with DNA polymerase epsilon. Nucleic Acids Res. **31:**5568–5575.
51. **Raj, K., P. Ogston, and P. Beard.** 2001. Virus-mediated killing of cells that lack p53 activity. Nature **412:**914–917.
52. **Rodriguez, M., X. Yu, J. Chen, and Z. Songyang.** 2003. Phosphopeptide binding specificities of BRCA1 COOH-terminal (BRCT) domains. J. Biol. Chem. **278:**52914–52918.
53. **Roos-Mattjus, P., K. M. Hopkins, A. J. Oestreich, B. T. Vroman, K. L. Johnson, S. Naylor, H. B. Lieberman, and L. M. Karnitz.** 2003. Phosphorylation of human Rad9 is required for genotoxin-activated checkpoint signaling. J. Biol. Chem. **278:**24428–24437.
54. **Roos-Mattjus, P., B. T. Vroman, M. A. Burtelow, M. Rauen, A. K. Eapen, and L. M. Karnitz.** 2002. Genotoxin-induced Rad9-Hus1-Rad1 (9-1-1) chromatin association is an early checkpoint signaling event. J. Biol. Chem. **277:**43809–43812.
55. **Roshal, M., B. Kim, Y. Zhu, P. Nghiem, and V. Planelles.** 2003. Activation of the ATR-mediated DNA damage response by the HIV-1 viral protein R. J. Biol. Chem. **278:**25879–25886.
56. **Saka, Y., F. Esashi, T. Matsusaka, S. Mochida, and M. Yanagida.** 1997. Damage and replication checkpoint control in fission yeast is ensured by interactions of Crb2, a protein with BRCT motif, with Cut5 and Chk1. Genes Dev. **11:**3387–3400.
57. **Salvetti, A., S. Oreve, G. Chadeuf, D. Favre, Y. Cherel, P. Champion-Arnaud, J. David-Ameline, and P. Moullier.** 1998. Factors influencing recombinant adeno-associated virus production. Hum. Gene Ther. **9:**695–706.
58. **Sambrook, J., E. F. Fritsch, and T. Maniatis.** 1989. Molecular cloning: a laboratory manual, 2nd ed. Cold Spring Harbor Laboratory Press, Cold Spring Harbor, N.Y.
59. **Scully, R., J. Chen, A. Plug, Y. Xiao, D. Weaver, J. Feunteun, T. Ashley, and D. M. Livingston.** 1997. Association of BRCA1 with Rad51 in mitotic and meiotic cells. Cell **88:**265–275.
60. **Scully, R., S. Ganesan, K. Vlasakova, J. Chen, M. Socolovsky, and D. M. Livingston.** 1999. Genetic analysis of BRCA1 function in a defined tumor cell line. Mol. Cell **4:**1093–1099.
61. **Sengupta, S., S. P. Linke, R. Pedeux, Q. Yang, J. Farnsworth, S. H. Garfield, K. Valerie, J. W. Shay, N. A. Ellis, B. Wasylyk, and C. C. Harris.** 2003. BLM helicase-dependent transport of p53 to sites of stalled DNA replication forks modulates homologous recombination. EMBO J. **22:**1210–1222.
62. **Sogo, J., A. Stasiak, W. DeBernardin, R. Losa, and T. Koller.** 1987. Binding of proteins to nuclear acids as studied by electron microscopy, p. 61-79. *In* J. Sommerville and U. Scheer (ed.), Electron microscopy in molecular biology. Biology IRL Press, Oxford, United Kingdom.
63. **Stasiak, A., and E. H. Egelman.** 1994. Structure and function of RecA-DNA complexes. Experientia **50:**192-203.
64. **St. Onge, R. P., C. M. Udell, R. Casselman, and S. Davey.** 1999. The human G2 checkpoint control protein hRAD9 is a nuclear phosphoprotein that forms complexes with hRAD1 and hHUS1. Mol. Biol. Cell **10:**1985–1995.
65. **Tang, J. Y., B. J. Hwang, J. M. Ford, P. C. Hanawalt, and G. Chu.** 2000. Xeroderma pigmentosum p48 gene enhances global genomic repair and suppresses UV-induced mutagenesis. Mol. Cell **5:**737-744.
66. **Tibbetts, R. S., D. Cortez, K. M. Brumbaugh, R. Scully, D. Livingston, S. J. Elledge, and R. T. Abraham.** 2000. Functional interactions between BRCA1 and the checkpoint kinase ATR during genotoxic stress. Genes Dev. **14:** 2989-3002.
67. **Volkmer, E., and L. M. Karnitz.** 1999. Human homologs of *Schizosaccharomyces pombe* Rad1, Hus1, and Rad9 form a DNA damage-responsive protein complex. J. Biol. Chem. **274:**567-570.
68. **Wakasugi, M., A. Kawashima, H. Morioka, S. Linn, A. Sancar, T. Mori, O. Nikaido, and T. Matsunaga.** 2002. DDB accumulates at DNA damage sites immediately after UV irradiation and directly stimulates nucleotide excision repair. J. Biol. Chem. **277:**1637-1640.
69. **Wang, H., and S. J. Elledge.** 2002. Genetic and physical interactions between DPB11 and DDC1 in the yeast DNA damage response pathway. Genetics **160:**1295-1304.
70. **Weiss, R. S., P. Leder, and C. Vaziri.** 2003. Critical role for mouse Hus1 in an S-phase DNA damage cell cycle checkpoint. Mol. Cell. Biol. **23:**791-803.
71. **Winocour, E., M. Callaham, and E. Huberman.** 1988. Perturbation of the cell cycle by adeno-associated virus. Virology **167:**393-399.
72. **Xiao, Z., Z. Chen, A. H. Gunasekera, T. J. Sowin, S. H. Rosenberg, S. Fesik, and H. Zhang.** 2003. Chk1 mediates S and G_2 arrests through Cdc25A degradation in response to DNA-damaging agents. J. Biol. Chem. **278:**21767-21773.
73. **Xu, B., A. H. O'Donnell, S. T. Kim, and M. B. Kastan.** 2002. Phosphorylation of serine 1387 in Brca1 is specifically required for the Atm-mediated S-phase checkpoint after ionizing irradiation. Cancer Res. **62:**4588-4591.
74. **Yamane, K., J. Chen, and T. J. Kinsella.** 2003. Both DNA topoisomerase II-binding protein 1 and BRCA1 regulate the G_2-M cell cycle checkpoint. Cancer Res. **63:**3049-3053.
75. **Yamane, K., X. Wu, and J. Chen.** 2002. A DNA damage-regulated BRCT-containing protein, TopBP1, is required for cell survival. Mol. Cell. Biol. **22:**555-566.
76. **Yamane, K., M. Kawabata, and T. Tsuruo.** 1997. A DNA-topoisomerase-II-binding protein with eight repeating regions similar to DNA-repair enzymes and to a cell-cycle regulator. Eur. J. Biochem. **250:**794-799.
77. **Yarden, R. I., S. Pardo-Reoyo, M. Sgagias, K. H. Cowan, and L. C. Brody.**

2002. BRCA1 regulates the G2/M checkpoint by activating Chk1 kinase upon DNA damage. Nat. Genet. **30:**285-289.
78. **You, Z., L. Kong, and J. Newport.** 2002. The role of single-stranded DNA and polymerase alpha in establishing the ATR, Hus1 DNA replication checkpoint. J. Biol. Chem. **277:**27088-27093.
79. **Yu, X., C. C. Chini, M. He, G. Mer, and J. Chen.** 2003. The BRCT domain is a phospho-protein binding domain. Science **302:**639-642.
80. **Yuan, R., S. Fan, M. Achary, D. M. Stewart, I. D. Goldberg, and E. M. Rosen.** 2001. Altered gene expression pattern in cultured human breast cancer cells treated with hepatocyte growth factor/scatter factor in the setting of DNA damage. Cancer Res. **61:**8022-8031.
81. **Zachos, G., M. D. Rainey, and D. A. Gillespie.** 2003. Chk1-deficient tumour cells are viable but exhibit multiple checkpoint and survival defects. EMBO J. **22:**713-723.
82. **Ziv, Y., A. Bar-Shira, I. Pecker, P. Russell, T. J. Jorgensen, I. Tsarfati, and Y. Shiloh.** 1997. Recombinant ATM protein complements the cellular A-T phenotype. Oncogene **15:**159-167.
83. **Zou, L., D. Cortez, and S. J. Elledge.** 2002. Regulation of ATR substrate selection by Rad17-dependent loading of Rad9 complexes onto chromatin. Genes Dev. **16:**198-208.
84. **Zou, L., and S. J. Elledge.** 2003. Sensing DNA damage through ATRIP recognition of RPA-ssDNA complexes. Science **300:**1542-1548.